

Research Article

Grain Size Dependence of Elastic Moduli in Nanocrystalline Tungsten

P. Valat-Villain, J. Durinck, and P. O. Renault

Department of Physics and Mechanics of Materials, Institut Pprime, UPR 3346 CNRS, Université de Poitiers, ENSMA, Futuroscope, SP2MI, BP 30179, 86962 Chasseneuil-du-Poitou, France

Correspondence should be addressed to P. Valat-Villain; pascale.valat@univ-poitiers.fr

Received 31 January 2017; Accepted 16 May 2017; Published 7 June 2017

Academic Editor: Ping Xiao

Copyright © 2017 P. Valat-Villain et al. This is an open access article distributed under the Creative Commons Attribution License, which permits unrestricted use, distribution, and reproduction in any medium, provided the original work is properly cited.

Using atomistic calculations with a Finnis-Sinclair type potential and molecular statics and dynamics methods, we performed a series of deformation tests on nanocrystallised tungsten samples presenting various microstructures; we calculated the elastic constants of polycrystalline tungsten for average grain diameters ranging from 2.7 to 6.7 nm. The results show that both Young's and the shear moduli decrease by over 60% as the average grain diameter decreases below 3 nm. This diminution appears to be highly correlated to the grain boundary volume fraction. The results are compared to conclusions from other authors.

1. Introduction

Mechanical properties of metals can dramatically change when their size scale becomes nanometric, this scale being the average grain diameter of a polycrystalline sample or the thickness of a thin layer [1–4]. In fact, in bulk nanocrystalline (nc) materials or in thin films, the volume fraction of the interfaces or/and surfaces becomes comparable to the volume fraction of the crystals. This relative microstructural evolution combined with the intrinsic volume decrease of crystalline parts can justify the significant changes observed for the mechanical behaviour of nanocrystalline materials.

Concerning the elastic behaviour, experimental measurements have shown that the elastic moduli of nanocrystalline metallic materials are substantially lower than those of their coarse-grained counterparts [5, 6]. The variation of elastic moduli may be attributed both to the large volume fraction of atoms that are located at interfaces and/or surfaces in nanocrystalline materials and to porosity [6–8]. Those authors have shown that small decrements from coarse-grained values observed in Young's modulus are caused primarily by the slight amount of porosity in the samples. The porosity found in most nanocrystalline materials, that is, not only the “missing grain” pores but also vacancy-sized pores detected by positron lifetime experiments, may be the analogy of the free volume in the amorphous metals [8].

More recent experiments on nanocrystalline Ni-P alloys have evidenced a grain size dependence of elastic moduli in fully dense samples [9, 10]. Other experiments have found that Young's modulus of the nc-Fe was essentially the same as that of coarse-grained Fe (8–33 nm) [11].

Since the 1990s, in addition to experimental measurements, computer simulations on the same subject have appeared in the literature. For example, in nc-Cu [12, 13], nc-Fe [14], and nc-Ni [15], a significant decrease of elastic moduli with decreasing grain size was reported.

However, most of these simulation studies are mainly dealing with plasticity [1, 12, 13, 16–20]. In a few cases the elastic domain is briefly mentioned before a detailed analysis of plasticity. Moreover, many studies deal with face centred cubic (fcc) metals such as nickel and copper, and only a few ones concern body centred cubic (bcc) transition metals such as α -iron [14, 21] and tantalum [22]. We believe that the technological importance of many bcc metals and our current poor knowledge of their elastic properties justify further investigation. Among bcc transition metals, tungsten offers particularly interesting applications in the microelectronic domain and to our knowledge, the elastic constants of nanocrystalline tungsten have not been studied yet. In a previous study [23] we have shown that surface effects can strongly influence the elastic properties of thin tungsten

TABLE 1: Mean grain size, grain centre distribution, grain boundary atomic fraction η , bulk modulus B , shear modulus μ , Young’s modulus E , and Poisson’s ratio ν , calculated from the above values of B and μ , and average values of Young’s modulus resulting from uniaxial strain tests, for each of the 8 samples studied in this paper. The bulk modulus for tungsten single crystal is 310 GPa with the potential used here, the shear modulus value is 161 GPa, Young’s modulus value is 410 GPa, and Poisson’s ratio value is 0.28.

Sample number	1	2	3	4	5	6	7	8
d_g (nm)	2.7	2.7	3.0	3.0	4.0	4.0	6.7	6.7
Grain centre distribution	BCC	FCC	BCC	FCC	BCC	FCC	BCC	FCC
Grain boundary atomic fraction η (%)	84	86	78	79	63	67.5	40	42
B (GPa)	221	229	235	232	249	245	269	268
B (GPa) before relaxation	276	274	277	278	289	286	299	299
μ (GPa)	61	58.5	65	63	75	74	100	106
μ (GPa) before relaxation	139	138	141	139	144	144	153	158
ν from B and μ	0.374	0.379	0.374	0.376	0.360	0.374	0.330	0.325
E (GPa) from B and μ	167	161	178	173	204	202	267	281
E (GPa) from uniaxial tests	165	162	178	173	207	202	270	285.5

single crystal layers. The question of grain size effects still remained; the present study aims to answer this question by investigating bulk nanocrystalline tungsten of different grain sizes. Tungsten single crystal is locally elastically isotropic; it is then possible to distinguish size effects from any texture effects in polycrystals.

2. Computational Details

2.1. Sample Preparation. As in our previous study [23], we used a Finnis-Sinclair type potential parametrised for tungsten by Ackland and Thetford [24, 25] that correctly reproduces interactions with surfaces, even at a nanometre scale. The simulation itself used cubic cells (referred below as “samples”) divided by means of a Voronoi method and repeated by periodic boundary conditions. In order to have a consistent uncertainty on the computed elastic moduli, the impact of sample elaboration on elastic moduli was examined by testing two different grain distributions and three different relaxation processes.

For each sample, the grain centres were uniformly placed on the nodes of a bcc lattice or a fcc lattice, giving all the grains a homogenous shape and size. For a given grain size, these two types of distribution were used in order to track any influence of the microstructure on the elastic properties. For each grain, the crystallographic orientation was randomly determined. Actually we built eight samples, containing 26000 to 234000 atoms with mean grain sizes (d_g) ranging from 2.7 to 6.7 nm (Table 1).

These samples were then relaxed by means of a molecular dynamics method (XMD code [26]), composed of annealing followed by quenching and a simple gradient relaxation at 0 K. The volume of each sample was then adjusted in order to minimize the cohesion energy. Relaxation was regarded as complete when the maximal residual force was lower than 10^{-3} eV/Å; the same criterion was used for all further relaxations. Three annealing routes were used for each sample, with temperatures ranging from 500 K to 2000 K. The first one consisted of one single annealing of 160 picoseconds

at 500 K (about $0.14 T_m$, where T_m is the melting point of tungsten), the second one was composed of 80 ps annealing at 1000 K ($0.27 T_m$) followed by 80 ps one at 500 K, and the third process was composed of four 40 ps annealing stages at the following temperatures: 2000 K ($0.54 T_m$), 1500 K, 1000 K, and 500 K. Figure 1 displays the evolution of the potential energy in sample number 3 ($d_g = 3.0$ nm) during the three annealing routes. The inset shows that, at the end of the final static relaxation, the three energies are very close to each other but not exactly equal, denoting small microstructure differences between the three relaxed configurations. Nevertheless, the annealing process turned out to have only marginal influence on the calculated elastic moduli, within the calculation uncertainties.

Figure 2 shows one of the relaxed samples; it was performed by means of the AtomEye software [27]; atoms are coloured according to the value of their coordination number taking into account the first and second neighbours. A cut-off radius slightly above the 2nd neighbour distance in W single crystal (0.322 nm) was chosen to count these neighbours.

Finally, we evaluated the influence of the grain size and the annealing process on grain boundaries. The grain boundary atomic fraction (η) was estimated by counting the over- or undercoordinated atoms and calculating their proportion regarding the total amount of atoms in the whole sample. η ranges from 40% for $d_g = 6.7$ nm up to 85% for $d_g = 2.7$ nm: the lower the average grain diameter, the higher the η value. Concerning the annealing process, we found that it only had slight influence on η . Table 1 reports η averages on the three annealing routes for each sample.

2.2. Elastic Constant Calculation. Deformation tests were performed at 0 K by imposing a linear or affine transformation to all the atom positions, followed by a simple gradient relaxation. First, the samples were submitted to isotropic compression and dilatation tests to determine the bulk modulus B . They were then tested with shear strain along three different directions in order to evaluate their shear modulus μ and to verify the macroscopic sample isotropy. Using the

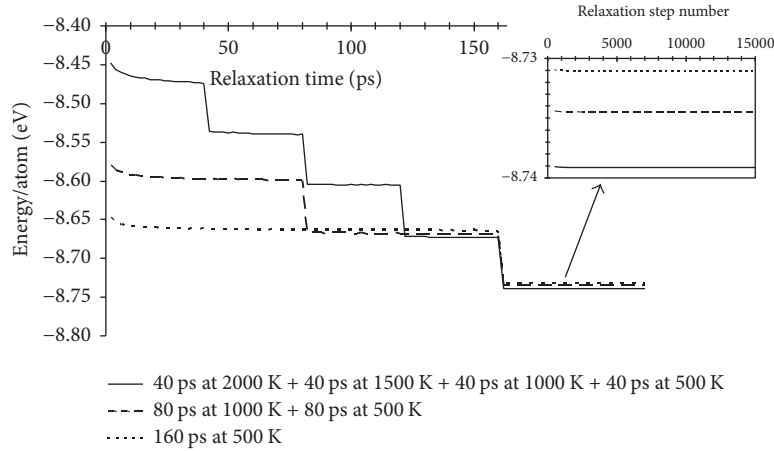


FIGURE 1: Evolution of the potential energy in sample number 3 ($d_g = 3.0$ nm) as a function of time during the three annealing routes. The inset displays the final static relaxation at 0 K.

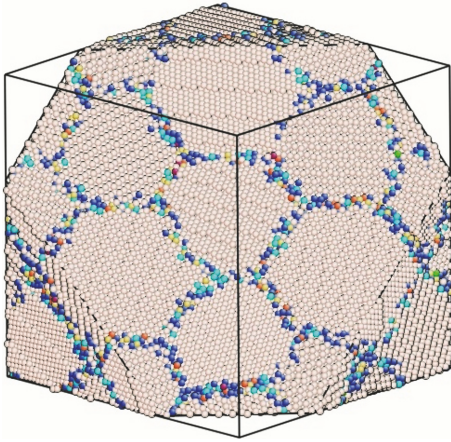


FIGURE 2: Relaxed sample with 16 grains of average grain diameter $d_g = 6.7$ nm. Atoms are coloured according to the value of their coordination number taking into account the first and second neighbours (white: bulk atoms with coordination number = 14; other colours: intercrystalline atoms).

relationships between the elastic moduli for an isotropic material, we deduced Young's modulus $E = 9B/(3B + \mu)$ and Poisson's ratio $\nu = (3B - 2\mu)/(6B + 2\mu)$. Young's modulus was also calculated directly from uniaxial tensile and compressive tests. The applied main strains were taken between -1% and $+1\%$ with a deformation step of 0.1% . Values of B , μ , and E were calculated for each sample by performing a second-order polynomial fit on the (energy, strain) plots. Since the three relaxation process gave similar values for the elastic moduli, only average values for each sample are displayed in Table 1. We also derived values of B and μ for each considered polycrystalline sample just after having applied the initial homogeneous deformation, before relaxation. These values do not reflect the real nanocrystalline material behaviour as it is believed that deformation should not remain homogeneously distributed in samples but they

help us to gain more insight in the behaviour of grain boundaries under strain. Finally, for each elastic constant, uncertainties were evaluated by computing the standard deviation (σ) of all values obtained for a given grain size with all samples and strain directions. Error bars were then fixed to 2σ , that is, a relative uncertainty of 2% for B and 10% for μ and E .

3. Results and Discussion

3.1. Elastic Constant Variations. The results displayed in Table 1 show that the bulk modulus decreases from 13% up to 28% in comparison with the single crystal, for grain diameter ranging, respectively, from 6.7 down to 2.7 nm. The shear modulus decreases by up to 62% in comparison with the single crystal, as the average grain diameter decreases down to 2.7 nm. One can note that the higher the grain boundary atomic fraction, the lower the shear modulus. Furthermore, the decrease of the shear modulus is more important than the one of the bulk modulus. If we consider the "nonrelaxed" values, variations with the grain size are much smaller. The "nonrelaxed" shear modulus decreases by only 14% in comparison with the single crystal, for the smallest grain size, and is almost equal to the single crystal one for the 6.7 nm grain diameter. The variations relative to the single crystal value are virtually the same for the "nonrelaxed" bulk modulus. In addition, differences between "relaxed" and "nonrelaxed" values are larger for μ than for B . Values of Poisson's ratio and Young's modulus deduced from the average values of B and μ are given in Table 1 together with the values of E resulting from uniaxial strain tests. The results from both methods are totally consistent and clearly demonstrate that Young's modulus of polycrystalline tungsten, like its shear modulus, decreases strongly as the average grain diameter decreases. The E/E_0 ratio, where E is the average value for each sample and E_0 the single crystal Young's modulus, is plotted in Figure 3 as a function of d_g . We can also notice that, on the opposite, Poisson's ratio increases as the average grain diameter decreases.

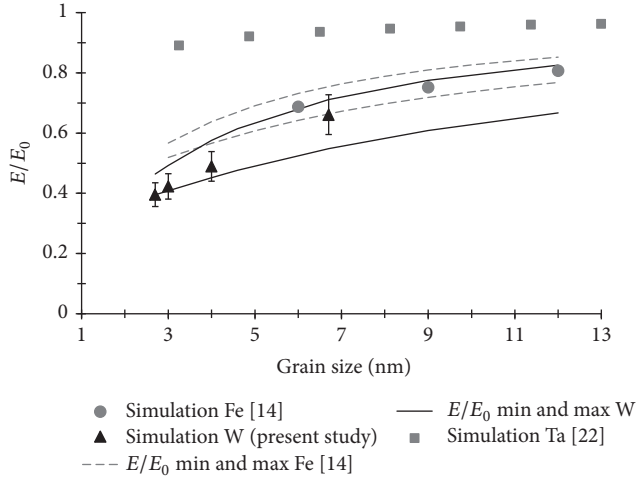


FIGURE 3: Ratio between Young's moduli in bcc nanocrystalline metals and the one of the corresponding single crystal as a function of grain size for calculated values in tungsten (\blacktriangle), calculated (\bullet) values in α -iron [14], calculated (\blacksquare) values in Ta [22], and rules of mixture in W (black plain lines) and Fe [14] (grey dashed lines). Rules of mixture were calculated with $E_{IC}/E_0 = 0.35$ for W, $E_{GB}/E_0 = 0.45$, and $E_{T1}/E_0 = 0.50$ for Fe.

3.2. Comparison with Literature and Interpretation. The grain size dependence of Young's modulus and the bulk modulus observed here in the case of a bcc metal (tungsten) can be related to studies that have given similar results for nanocrystalline fcc metals. Based on molecular dynamics simulations on polycrystalline Cu with a grain size of 4.3 nm, Phillpot et al. [12] obtained a Young's modulus decrease equal to 27% of the coarse-grained material value while the decrease of the bulk modulus was only equal to 8% of the polycrystalline average value. Schiötz et al. [13] reported a Young's modulus decrease of about 30% for nc-copper at 0 K with mean grain sizes down to 3.3 nm. Zhao et al. [15] have studied more precisely the grain size dependence of the bulk modulus of nc nickel. They observed a small reduction of B (up to 7%) when the grain size decreases from 40 down to 3 nm. In the case of bcc metals, Latapie and Farkas [14] studied nc α -iron with grain size ranging from 6 to 12 nm and observed a decrease of Young's modulus attaining 30% (compared to the bulk value) for $d_g = 6$ nm. But, more recently, Pan et al. [22] reported a much smaller dependence of Young's modulus, that is, a decrease of only 10% for 3.25 nm grain size in nc-Ta.

Thus our study confirms qualitatively the decrease of elastic moduli with the reduction of grain size down to a few nanometers. Furthermore we observed that while the decrease of Young's modulus is very large, the decrease of B is moderate, similarly to Phillpot et al. [12] in nc-copper. As already noticed by Zhao et al. [15], it should be noted that the initial grain size distribution has no obvious influence on elastic constants; these ones rather seem to depend mainly on the grain boundary atomic fraction. This point suggests that the elastic modulus variations observed here are mainly due to the grain boundary contribution. Density or porosity effects are also often invoked to account for the softening

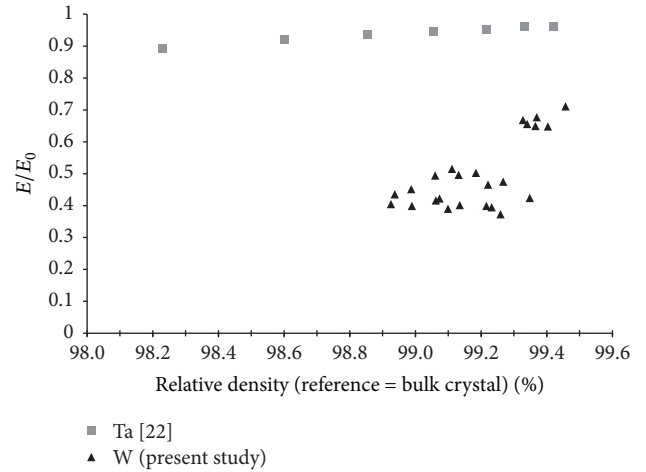


FIGURE 4: Ratio between Young's moduli in bcc nanocrystalline metals and the one of the corresponding single crystal as a function of the relative density, for calculated values in tungsten (\blacktriangle) and calculated (\blacksquare) values in Ta [22].

observed in nc materials [7, 8, 22]. However in our case, density is almost constant and very close to the bulk one (between 98.9% and 99.5%). The E/E_0 ratio, where E is the calculated value for each tungsten sample and each deformation test and E_0 the single crystal Young's modulus, is plotted in Figure 4 as a function of the density of the sample (in percentage of the bulk one). The values for tantalum [22] are also reported in this figure. In the case of tungsten, contrary to the case of tantalum, no clear correlation can be established between the density and E so that no porosity effect can be involved. Consequently, the tungsten softening observed in our study should be essentially accounted for by the high fraction of grain boundary regions and their particular deformation behaviour, as also suggested by Latapie and Farkas [14] for nc iron and Schiötz et al. [13] for nc-copper. The comparison between the "relaxed" and "nonrelaxed" values of B and μ suggests that nonaffine deformation takes place in grain boundary regions, leading to an additional decrease of the elastic constants. The bulk modulus appears to be less sensitive than the shear modulus to the relaxation that occurs after the application of the homogeneous strain. This can be explained by the fact that a shear strain is more likely to destabilize the atomic arrangement and induce nonaffine and/or plastic deformation at grain boundaries than an isotropic strain. Moreover, because nonaffine motion of atoms at grain boundaries is probably thermally activated, it is believed that the grain size effect on the shear modulus (and thus Young's modulus) should be larger at finite temperature than at 0 K.

The main role played by the grain boundary regions can be confirmed by considering that a polycrystalline material is composed of an intercrystalline "phase" (i.e., grain boundaries, triple junctions, and quadruple nodes) and a crystal "phase" (i.e., grain interior) [6, 14, 28–30]. In such a rule of mixture model, the in-grain regions present a Young's modulus similar to the bulk material while the intercrystalline

(IC) regions present a smaller one. This was, for instance, confirmed by the molecular dynamics simulations performed recently by Lian et al. on bulk nanocrystalline nickel [31].

Thus an upper (E_{\max}) and a lower (E_{\min}) limit for Young's modulus may be calculated by means of the following equations:

$$\begin{aligned} \frac{E_{\max}}{E_0} &= (1 - V_{\text{GB}} - V_{\text{TJ}}) + V_{\text{GB}} \frac{E_{\text{GB}}}{E_0} + V_{\text{TJ}} \frac{E_{\text{TJ}}}{E_0} \\ \frac{E_0}{E_{\min}} &= (1 - V_{\text{GB}} - V_{\text{TJ}}) + \frac{V_{\text{GB}}}{E_{\text{GB}}/E_0} + \frac{V_{\text{TJ}}}{E_{\text{TJ}}/E_0}, \end{aligned} \quad (1)$$

where V_{GB} and V_{TJ} are the volume fractions of the grain boundaries and triple junctions, respectively, E_{GB} and E_{TJ} are Young's moduli of the grain boundary and triple junction components, respectively, and E_0 is Young's modulus of the perfect crystal lattice [6, 14]. In our case, as the sample density is constant and very close to the bulk one, the atomic volume is assumed to be the same in grain interior and intercrystalline phases. It comes then that $\eta = V_{\text{GB}} + V_{\text{TJ}}$. Moreover no distinction is made between grain boundary and triple junction elastic moduli so that $E_{\text{GB}} = E_{\text{TJ}} = E_{\text{IC}}$. Given these assumptions, (1) may be rewritten as

$$\frac{E_{\max}}{E_0} = (1 - \eta) + \eta \frac{E_{\text{IC}}}{E_0} \quad (2)$$

$$\frac{E_0}{E_{\min}} = (1 - \eta) + \eta \frac{E_0}{E_{\text{IC}}}. \quad (3)$$

Figure 3 shows the results on α -iron extracted from [14] and the ones on tantalum extracted from [22], together with the present results on tungsten. The first striking point is that the relative values (E/E_0) of tungsten Young's modulus are consistent with those of iron for $d_g \approx 6$ nm while they are completely different from those of tantalum for similar grain sizes. Softening appears to be far much smaller in tantalum than in iron or tungsten. Concerning the upper and lower limits for the elastic modulus values, it is important to note that these analytical models include two parameters to determine η and E_{IC}/E_0 . The value of E_{IC}/E_0 cannot be extracted directly from our simulation technique since this one gives only an average value of E for the polycrystal. In literature, some authors like Shen et al. [6] chose to adopt the value of the amorphous counterpart material whereas other authors like Zhao et al. [15] evidenced that the grain boundary phase was elastically different from the amorphous state. The intercrystalline volume η may be evaluated either by an analytical model such as Palumbo's [28] or Kim's ones [30] wherein the grain boundary thickness Δ needs to be known or by a microstructural analysis of the computed samples. As already mentioned, we adopted the latter method. The choice of the cut-off radius for counting atomic neighbours results in a large uncertainty on the η parameter. Fitting our η values on Palumbo's equation for the total IC-volume gives a grain boundary thickness Δ of about 1.2 nm. This Δ value is similar to the ones used by Latapie and Farkas for α -iron (1.3 nm) [14], Zhao et al. for nickel (≈ 1 nm) [15], or Palumbo et al. themselves (1.0 nm) [28].

Assuming a GB thickness of 1.3 nm and E_{GB}/E_0 and E_{TJ}/E_0 values equal to 0.45 and 0.50, respectively, Latapie and Farkas [14] determined an upper and a lower limit for E/E_0 in α -iron. Their curves are reported in Figure 3 (grey dashed lines). It clearly appears that these limits cannot include tungsten values for the smaller grain sizes. Thus we fitted all tungsten and iron E/E_0 values on both (2) and (3). The upper and lower limits for the best fit value (i.e., $E_{\text{IC}}/E_0 = 0.35$) are also displayed in Figure 3 (black plain lines). Consequently, this simple rule of mixture analytical model leads to assume a 65% reduction of intercrystalline grain boundary Young's modulus. To our knowledge, such a decrease has never been observed in other metals so far.

4. Conclusion

To summarise, we have shown by means of atomistic simulations that Young's and shear moduli of nanocrystallised tungsten strongly decrease (by over 60%) when the average grain diameter decreases down to 2.7 nm. This large decrease cannot be explained by a porosity effect, but rather by the high grain boundary volume fraction in nanocrystallised samples, with grain boundary regions having a smaller modulus than in-grain parts of the crystal. The global elastic modulus evolution can be correctly described by a rule of mixture between the in-grain modulus and the intercrystalline modulus. The present results denote very low elastic moduli of grain boundary regions.

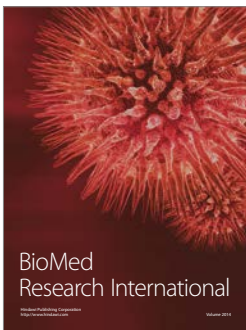
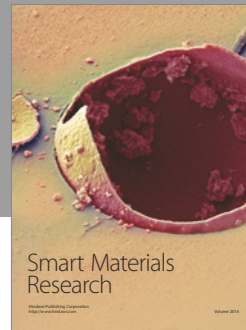
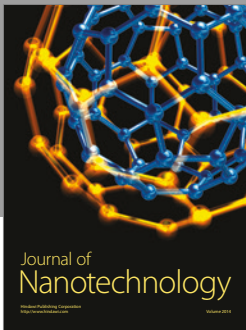
Conflicts of Interest

All authors declare that there are no conflicts of interest regarding the publication of this paper.

References

- [1] D. Wolf, V. Yamakov, S. R. Phillpot, A. Mukherjee, and H. Gleiter, "Deformation of nanocrystalline materials by molecular-dynamics simulation: relationship to experiments?" *Acta Materialia*, vol. 53, no. 1, pp. 1–40, 2005.
- [2] M. A. Meyers, A. Mishra, and D. J. Benson, "Mechanical properties of nanocrystalline materials," *Progress in Materials Science*, vol. 51, no. 4, pp. 427–556, 2006.
- [3] C. S. Pande and K. P. Cooper, "Nanomechanics of Hall-Petch relationship in nanocrystalline materials," *Progress in Materials Science*, vol. 54, no. 6, pp. 689–706, 2009.
- [4] E. Arzt, "Size effects in materials due to microstructural and dimensional constraints: a comparative review," *Acta Materialia*, vol. 46, no. 16, pp. 5611–5626, 1998.
- [5] V. Krstic, U. Erb, and G. Palumbo, "Effect of porosity on Young's modulus of nanocrystalline materials," *Scripta Metallurgica et Materialia*, vol. 29, no. 11, pp. 1501–1504, 1993.
- [6] T. D. Shen, C. C. Koch, T. Y. Tsui, and G. M. Pharr, "On the elastic moduli of nanocrystalline Fe, Cu, Ni, and Cu-Ni alloys prepared by mechanical milling/alloying," *Journal of Materials Research*, vol. 10, no. 11, pp. 2892–2896, 1995.
- [7] G. E. Fougere, L. Riester, M. Ferber, J. R. Weertman, and R. W. Siegel, "Young's modulus of nanocrystalline Fe measured by nanoindentation," *Materials Science and Engineering A*, vol. 204, no. 1–2, pp. 1–6, 1995.

- [8] P. G. Sanders, J. A. Eastman, and J. R. Weertman, "Elastic and tensile behavior of nanocrystalline copper and palladium," *Acta Materialia*, vol. 45, no. 10, pp. 4019–4025, 1997.
- [9] Y. Zhou, U. Erb, K. T. Aust, and G. Palumbo, "The effects of triple junctions and grain boundaries on hardness and Young's modulus in nanostructured Ni-P," *Scripta Materialia*, vol. 48, pp. 825–830, 2003.
- [10] Y. Zhou, U. Erb, and K. T. Aust, "The role of interface volume fractions in the nanocrystalline to amorphous transition in fully dense materials," *Philosophical Magazine*, vol. 87, no. 36, pp. 5749–5761, 2007.
- [11] T. R. Malow and C. C. Koch, "Mechanical properties in tension of mechanically attrited nanocrystalline iron by the use of the miniaturized disk bend test," *Acta Materialia*, vol. 46, no. 18, pp. 6459–6473, 1998.
- [12] S. R. Phillpot, D. Wolf, and H. Gleiter, "Molecular-dynamics study of the synthesis and characterization of a fully dense, three-dimensional nanocrystalline material," *Journal of Applied Physics*, vol. 78, no. 2, pp. 847–861, 1995.
- [13] J. Schiøtz, T. Vegge, F. D. Di Tolla, and K. W. Jacobsen, "Atomic-scale simulations of the mechanical deformation of nanocrystalline metals," *Physical Review B*, vol. 60, no. 17, pp. 11971–11983, 1999.
- [14] A. Latapie and D. Farkas, "Effect of grain size on the elastic properties of nanocrystalline α -iron," *Scripta Materialia*, vol. 48, no. 5, pp. 611–615, 2003.
- [15] S.-J. Zhao, K. Albe, and H. Hahn, "Grain size dependence of the bulk modulus of nanocrystalline nickel," *Scripta Materialia*, vol. 55, no. 5, pp. 473–476, 2006.
- [16] P. M. Derlet and H. Van Swygenhoven, "Length scale effects in the simulation of deformation properties of nanocrystalline metals," *Scripta Materialia*, vol. 47, no. 11, pp. 719–724, 2002.
- [17] A. C. Lund and C. A. Schuh, "Strength asymmetry in nanocrystalline metals under multiaxial loading," *Acta Materialia*, vol. 53, no. 11, pp. 3193–3205, 2005.
- [18] H. Van Swygenhoven and P. M. Derlet, "Grain-boundary sliding in nanocrystalline fcc metals," *Physical Review B*, vol. 64, no. 22, article 224105, 2001.
- [19] E. Bitzek, P. M. Derlet, P. M. Anderson, and H. Van Swygenhoven, "The stress-strain response of nanocrystalline metals: a statistical analysis of atomistic simulations," *Acta Materialia*, vol. 56, no. 17, pp. 4846–4857, 2008.
- [20] S. L. Frederiksen, K. W. Jacobsen, and J. Schiøtz, "Simulations of intergranular fracture in nanocrystalline molybdenum," *Acta Materialia*, vol. 52, no. 17, pp. 5019–5029, 2004.
- [21] D. Chen, "Computer model simulation study of nanocrystalline iron," *Materials Science and Engineering A*, vol. 190, no. 1-2, pp. 193–198, 1995.
- [22] Z. Pan, Y. Li, and Q. Wei, "Tensile properties of nanocrystalline tantalum from molecular dynamics simulations," *Acta Materialia*, vol. 56, no. 14, pp. 3470–3480, 2008.
- [23] P. Villain, P. Beauchamp, K. F. Badawi, P. Goudeau, and P.-O. Renault, "Atomistic calculation of size effects on elastic coefficients in nanometre-sized tungsten layers and wires," *Scripta Materialia*, vol. 50, no. 9, pp. 1247–1251, 2004.
- [24] G. J. Ackland and R. Thetford, "An improved N-body semi-empirical model for body-centred cubic transition metals," *Philosophical Magazine A*, vol. 56, no. 1, pp. 15–30, 1987.
- [25] M. W. Finnis and J. E. Sinclair, "A simple empirical N-body potential for transition metals," *Philosophical Magazine A*, vol. 50, no. 1, pp. 45–55, 1984.
- [26] <http://xmd.sourceforge.net/about.html>.
- [27] J. Li, "AtomEye: an efficient atomistic configuration viewer," *Modelling and Simulation in Materials Science and Engineering*, vol. 11, no. 2, pp. 173–177, 2003.
- [28] G. Palumbo, S. J. Thorpe, and K. T. Aust, "On the contribution of triple junctions to the structure and properties of nanocrystalline materials," *Scripta Metallurgica et Materialia*, vol. 24, no. 7, pp. 1347–1350, 1990.
- [29] J. E. Carsley, J. Ning, W. W. Milligan, S. A. Hackney, and E. C. Aifantis, "A simple, mixtures-based model for the grain size dependence of strength in nanophase metals," *Nanostructured Materials*, vol. 5, no. 4, pp. 441–448, 1995.
- [30] H. S. Kim, Y. Estrin, and M. B. Bush, "Plastic deformation behaviour of fine-grained materials," *Acta Materialia*, vol. 48, no. 2, pp. 493–504, 2000.
- [31] J. Lian, S.-W. Lee, L. Valdevit, M. I. Baskes, and J. R. Greer, "Emergence of film-thickness- and grain-size-dependent elastic properties in nanocrystalline thin films," *Scripta Materialia*, vol. 68, no. 5, pp. 261–264, 2013.



Hindawi

Submit your manuscripts at
<https://www.hindawi.com>

